FRG study of the phase diagram of the quark-meson model with vector interactions

Renan Câmara Pereira

Renan Câmara Pereira, Rainer Stiele, Pedro Costa, arXiv:2003.12829

Centre for Physics of the University of Coimbra

June 26, 2020

The QCD phase diagram

The different manifestations of QCD matter can be displayed in a $T - \mu_B$ phase diagram.

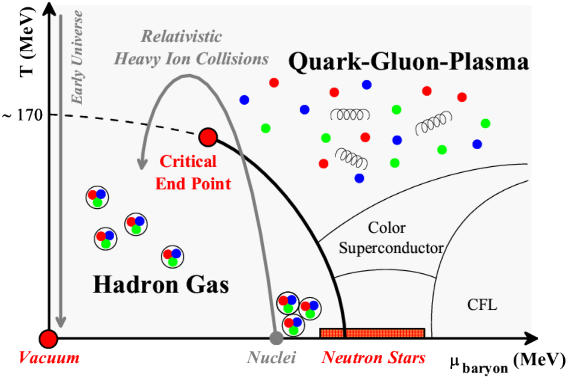

The theoretical study of the QCD phase diagram can be addressed within different approaches:

- **Lattice QCD**
  - first principle calculations;
  - currently only works on the finite temperature and zero/low density region due to the so called sign problem;

- **Dyson–Schwinger equations**
  - truncation required;

- **Effective models**
  - incorporate the most important features of QCD at a certain energy scale;
  - work on the entire range of the phase diagram;
  - coupling parameters need to be fixed to experimental data or first principle calculations;

We are interested in the low temperature, high density region of the phase diagram in which neutron stars evolve.

QCD effective models like Nambu−Jona-Lasinio or Quark-Meson models, are a great tools to study this region.

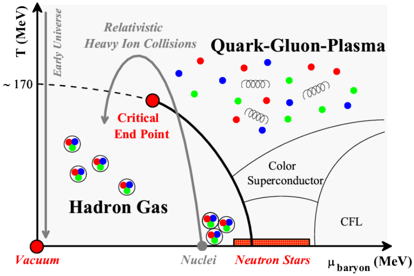

Such models are widely applied in the so-called mean field approximation. Only classical field configuration in the path integral is taken into account. Quantum fluctuations are left aside.

However, quantum fluctuations are important to correctly study the critical behaviour of the models (e.g. critical exponents).

In the present work we will study the low temperature, high chemical potential behaviour of the QM model, beyond the usual mean field approximation, to include quantum fluctuations using the Functional Renormalization Group, a non-perturbative method.

The Functional Renormalization Group

The central object in FRG is a scale-dependent (k), effective average action functional Γ_k, with the limits:

$$\begin{aligned} \Gamma_{k\longrightarrow\Lambda} &\simeq \mathcal{S}_0 \quad \text{The bare action to be quantized,} \\ \Gamma_{k\longrightarrow 0} &= \Gamma \quad \text{The action with all quantum fluctuations.} \end{aligned}$$

This functional must obey the Wetterich flow equation, an exact equation. For a scalar field it can be written as:

$$\partial_t \Gamma_k [\phi] = \frac{1}{2} \operatorname{tr} \left[\partial_t R_k \left(\Gamma_k^{(2)} [\phi] + R_k \right)^{-1} \right].$$

Here, R_k is called the regulator.

The $SU(2)_f$ Quark-Meson model

The QM model is built by considering a quark field, interacting with dynamical meson fields via chiral symmetry conserving terms i.e., $SU(2)_L \times SU(2)_R$. The Lagrangian density is:

$$\mathcal{L} = \overline{\psi}\left[i\partial\!\!\!/ - g_S(\sigma + i\boldsymbol{\tau}\cdot\boldsymbol{\pi}\gamma_5) - g_\omega \omega\!\!\!/ + \mu\gamma_0\right]\psi + \frac{1}{2}(\partial_\mu\sigma)^2 + \frac{1}{2}(\partial_\mu\boldsymbol{\pi})^2 - \frac{1}{4}F_{\mu\nu}F^{\mu\nu} - U(\sigma,\boldsymbol{\pi},\omega_\mu).$$

The field tensor $F_{\mu\nu}$ is used to define the kinetic terms for the ω_μ field,

$$F_{\mu\nu} = \partial_\mu\omega_\nu - \partial_\nu\omega_\mu.$$

The potential $U(\sigma,\boldsymbol{\pi},\omega_\mu)$, has to respect chiral symmetry. Explicit symmetry breaking can be included to mimic finite quark current masses.

We will freeze the vector degrees of freedom: only quantum fluctuations in the quark, π and σ mesons will be considered.

This procedure can be translated in the following restriction for the effective action:

$$\left.\frac{\partial \Gamma(\omega_\mu)}{\partial \omega_\mu}\right|_{\omega_\mu = \tilde{\omega}_\mu} = 0$$

Due to rotational invariance, the spatial components of the mean fields $\tilde{\omega}_j$, vanish. Only the field $\tilde{\omega}_0$ can be non-zero which can be absorbed in the definition of the effective quark chemical potential:

$$\tilde{\mu}_i = \mu_i - g_\omega \tilde{\omega}_0 .$$

Flow Equations: Potential

The dimensionful LPA flow equation for the effective potential $U_k^{\chi}(T,\tilde{\mu};\sigma)$ is:

$$\partial_t U_k^{\chi}(T,\tilde{\mu};\sigma) = \frac{k^5}{12\pi^2}\left\{ \frac{1}{E_\sigma}\left[1+2n_{\mathrm{B}}(E_\sigma)\right] + \frac{3}{E_\pi}\left[1+2n_{\mathrm{B}}(E_\pi)\right] - \frac{4N_c}{E_\psi}\sum_{i=u,d}\left(1-\sum_{\eta=\pm1} n_{\mathrm{F}}(E_\psi-\eta\tilde{\mu}_i)\right)\right\}.$$

Here, $n_{\mathrm{B}}(E)$ and $n_{\mathrm{F}}(E)$ are the Bose-Einstein and Fermi-Dirac distribution functions respectively and,

$$E_\sigma = \sqrt{k^2+\partial_\sigma^2 U_k^{\chi}}, \qquad E_\pi = \sqrt{k^2+\frac{\partial_\sigma U_k^{\chi}}{\sigma}}, \qquad E_\psi = \sqrt{k^2+g_S^2\sigma^2}.$$

The potential restriction w.r.t. ω_0, requires that, for each momentum shell k,

$$g_\omega\tilde{\omega}_{0,k} = g_\omega\tilde{\omega}_{0,\Lambda} + \frac{4N_c}{12\pi^2}\left(\frac{g_\omega}{m_\omega}\right)^2\sum_{i=u,d}\sum_{\eta=\pm1}\int_k^\Lambda \mathrm{d}p\,\frac{p^4}{E_\psi}\frac{\eta n_{\mathrm{F}}(E_\psi-\eta\tilde{\mu}_i)}{T}\left[1-n_{\mathrm{F}}(E_\psi-\eta\tilde{\mu}_i)\right].$$

The system of coupled partial differential equations, for the effective average potential, average entropy must be solved numerically alongside the self consistent equation for the $\tilde{\omega}_0$ vector field.

Two options:

- Taylor expansion around the scale-dependent minimum: not well suited to study the region of the phase diagram a first-order phase transition is expected and two minima co-exist.
- Grid method: provides full access to the effective potential, in a given range of the σ field.

In the later, the field variable σ is discretized in an one-dimensional grid, and the first and second derivatives of the effective potential w.r.t. σ are calculated using finite differences.

Results

The initial conditions for the partial differential equations are the following:

$$U_\Lambda(T,\tilde{\mu};\sigma) = \frac{1}{2}m_\Lambda^2\sigma^2 + \frac{1}{4}\lambda_\Lambda\sigma^4,$$
$$s_\Lambda(T,\tilde{\mu};\sigma) = 0,$$
$$g_\omega\tilde{\omega}_{0,\Lambda}(T,\tilde{\mu};\sigma) = 0.$$

Λ [MeV]	m_Λ/Λ	λ_Λ	c/Λ^3	g_S
1000	0.969	0.001	0.00175	4.2

Table: Used parameter set Tripolt et al., 2018. It yields in the vacuum, for $k_{\mathrm{IR}} = 80$ MeV, $f_\pi = 92.4$ MeV, $m_\pi = 137.6$ MeV, $m_\sigma = 606.7$ MeV and $m_q = 388.2$ MeV.

The ratio $g_\omega/m_\omega = G_\omega$ will be used as a free parameter bounded by $g_\omega = 1 - 20$ and $m_\omega \sim 1$ GeV. This means $G_\omega = 0.001 - 0.02$ MeV^{-1}.

Solving the vacuum flow: $T = 0$, $\mu_q = 0$

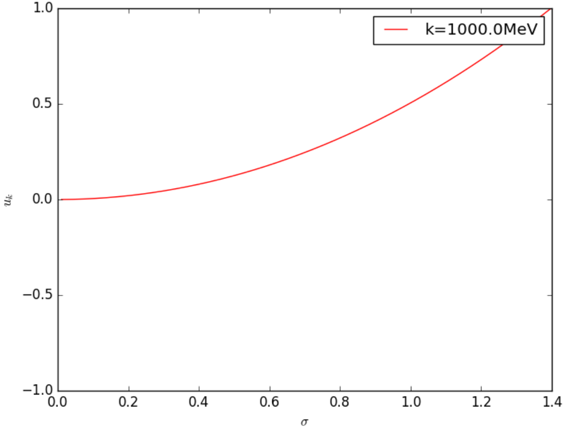

Solving the vacuum flow: $T = 0$, $\mu_q = 0$

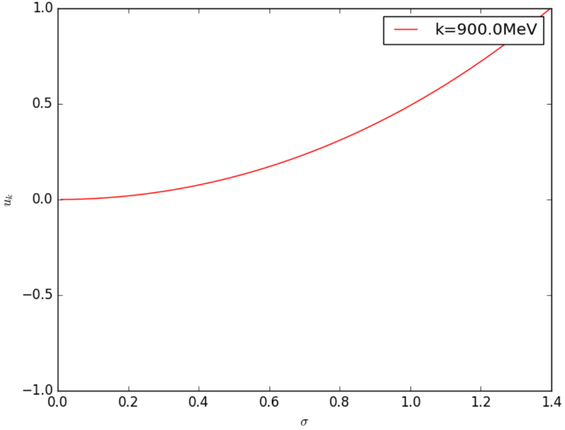

Solving the vacuum flow: $T = 0$, $\mu_q = 0$

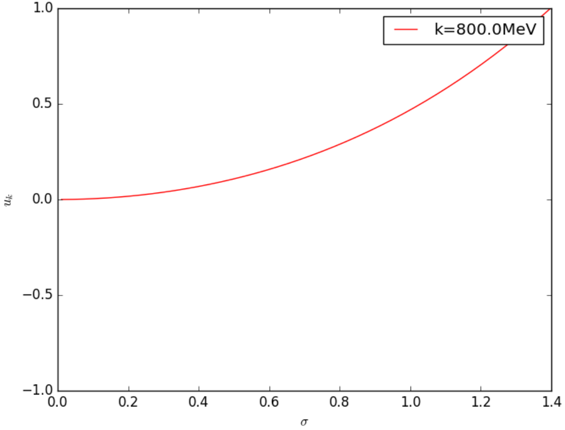

Solving the vacuum flow: $T = 0$, $\mu_q = 0$

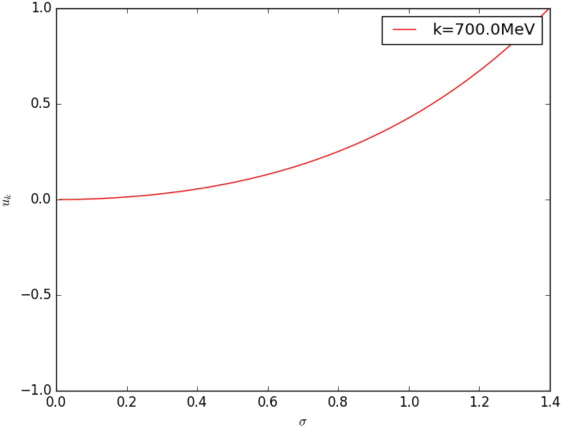

Solving the vacuum flow: $T = 0$, $\mu_q = 0$

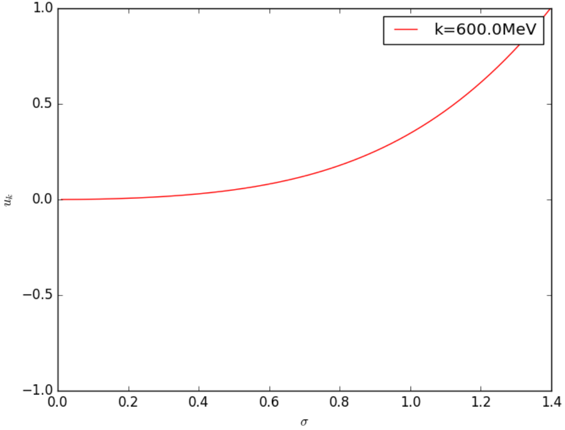

Solving the vacuum flow: $T = 0$, $\mu_q = 0$

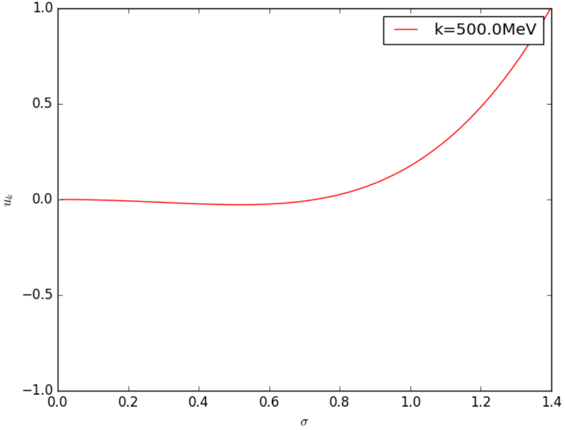

Solving the vacuum flow: $T = 0$, $\mu_q = 0$

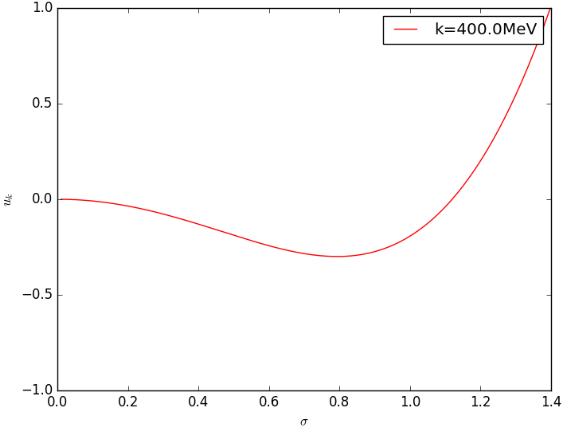

Solving the vacuum flow: $T = 0$, $\mu_q = 0$

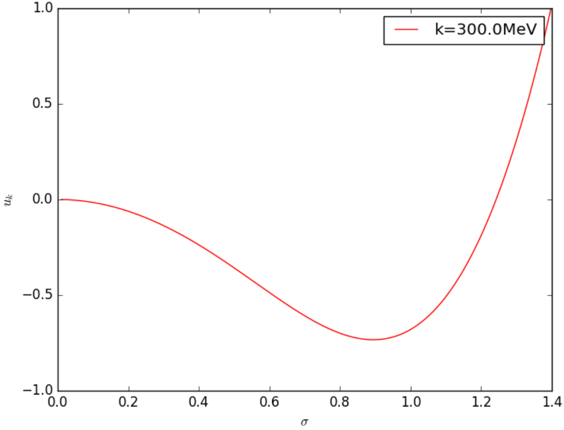

Solving the vacuum flow: $T = 0$, $\mu_q = 0$

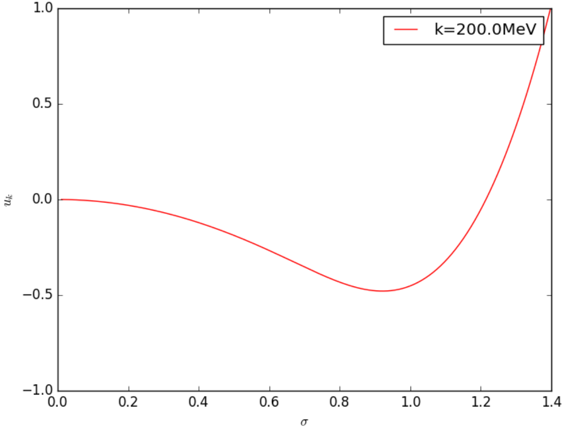

Solving the vacuum flow: $T = 0$, $\mu_q = 0$

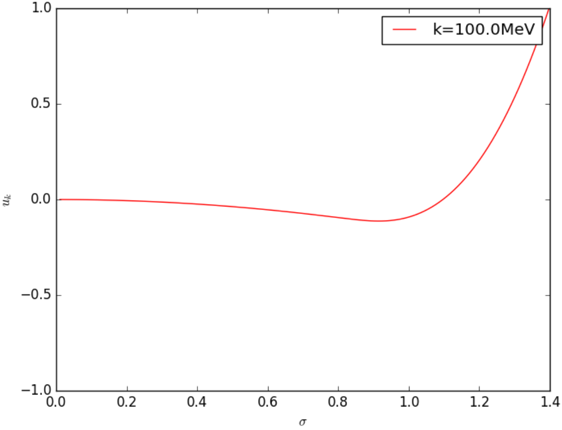

Solving the vacuum flow: $T = 0$, $\mu_q = 0$

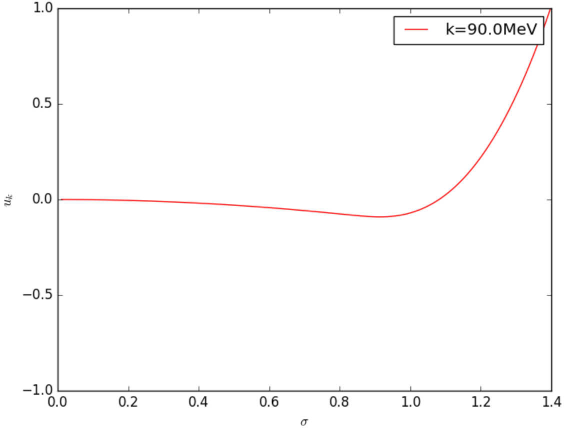

Solving the vacuum flow: $T = 0$, $\mu_q = 0$

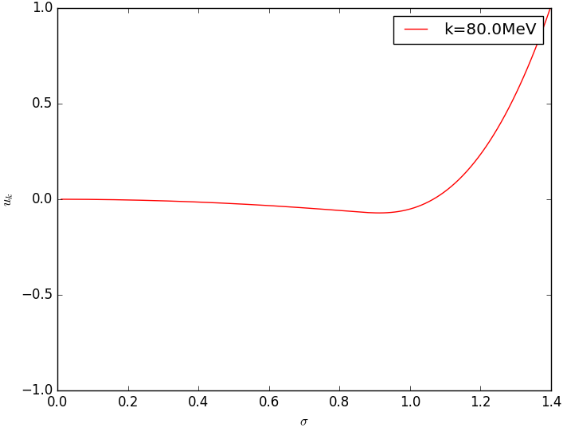

Solving the vacuum flow: $T = 0$, $\mu_q = 0$

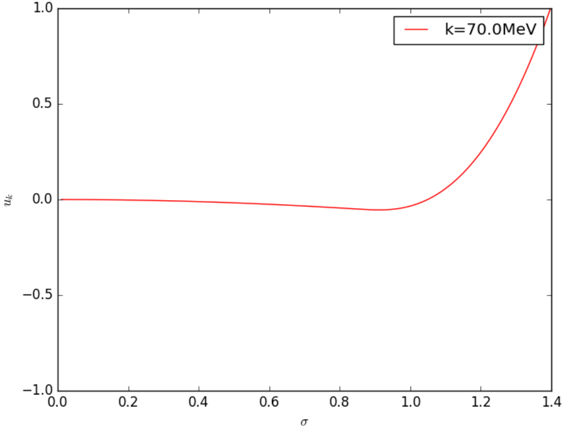

Solving the vacuum flow: $T = 0$, $\mu_q = 0$

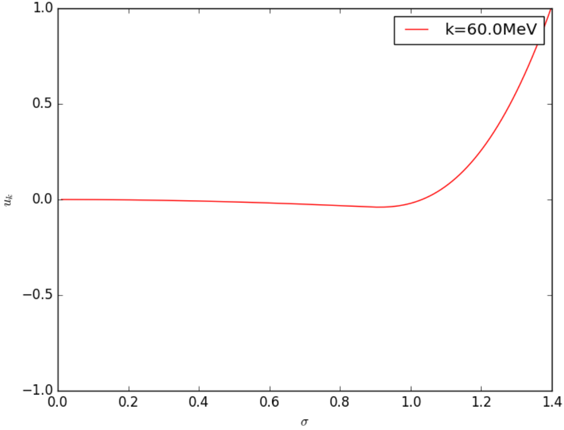

Solving the vacuum flow: $T = 0$, $\mu_q = 0$

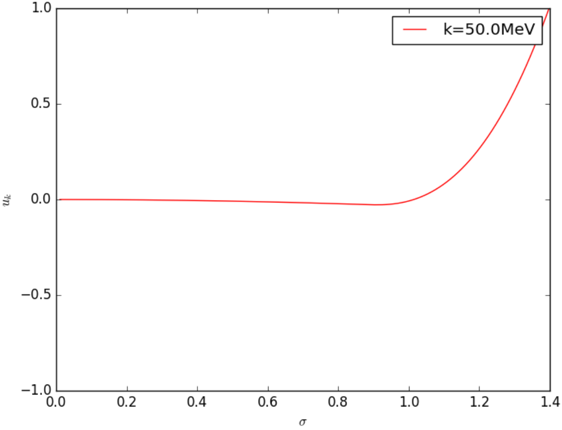

Solving the vacuum flow: $T = 0$, $\mu_q = 0$

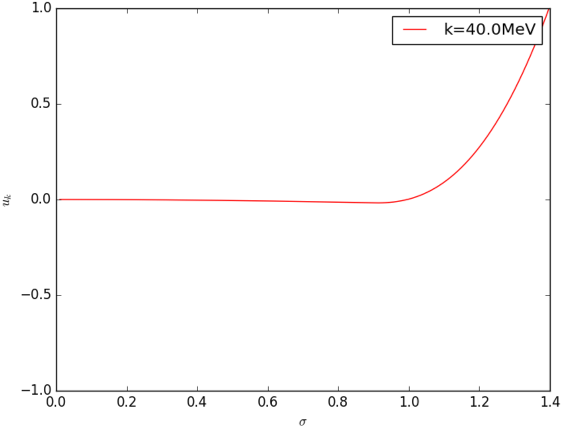

Drawing the Phase Diagram

- Solve the flow equations for several values of T and μ_q;
- Study the shape of the potential;
- Draw the phase diagram;

The chiral phase transition will be calculated with the Maxwell construction: when the effective potential has several minima, the one with lowest energy represents the stable phase

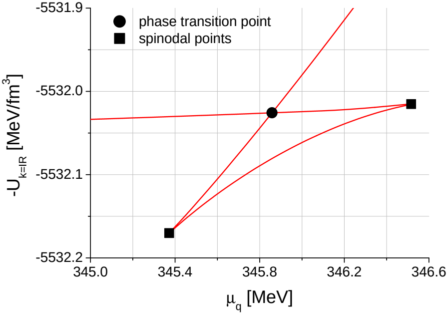

Phase Diagram: $k_{\mathrm{IR}} = 80$ MeV, $G_\omega = 0$

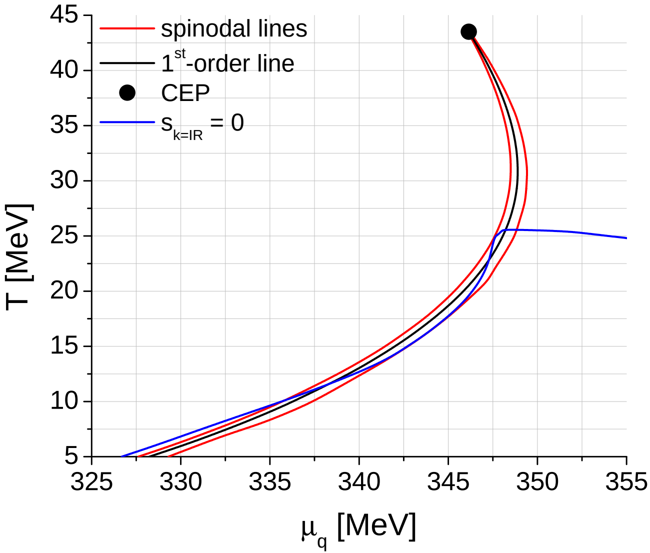

In Tripolt et al., 2018, it was found that the application of the FRG to the 2-flavour Quark-Meson leads to a negative entropy region near the first-order chiral transition of the model.

The authors have put forward some explanations for this unphysical region:

- The truncation used to derive the QM flow equation is not enough or the regulator is not appropriate;
- Transition to a color superconducting phase or to an inhomogeneous phase;

What is the effect of vector interactions in the phase transition and in the unphysical negative entropy region?

Phase Diagram: $k_{\mathrm{IR}} = 80$ MeV

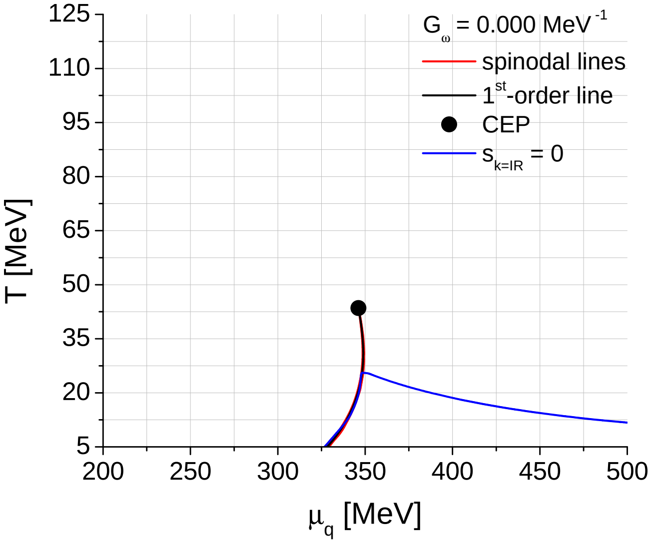

Phase Diagram: $k_{\mathrm{IR}} = 80$ MeV

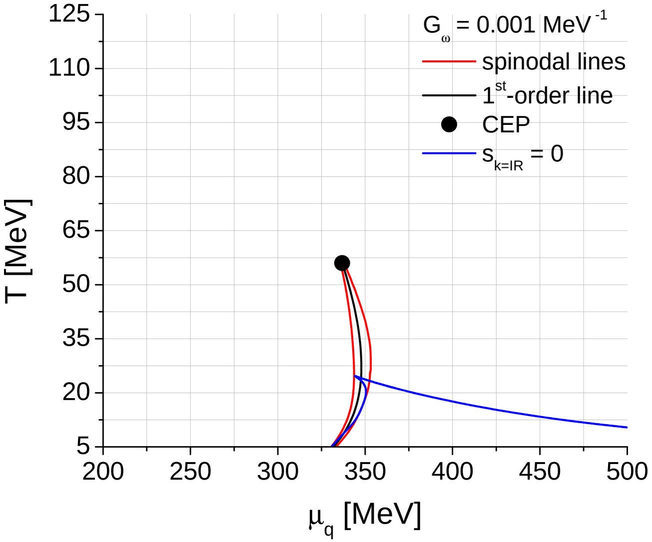

Phase Diagram: $k_{\rm IR} = 80$ MeV

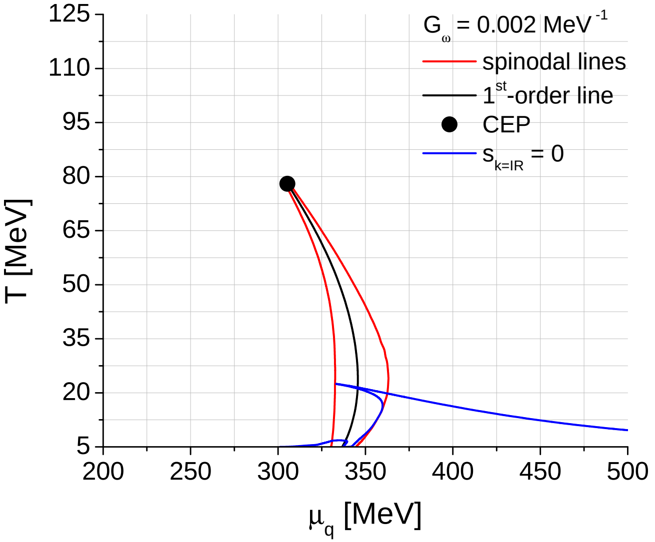

Phase Diagram: $k_{\mathrm{IR}} = 80$ MeV

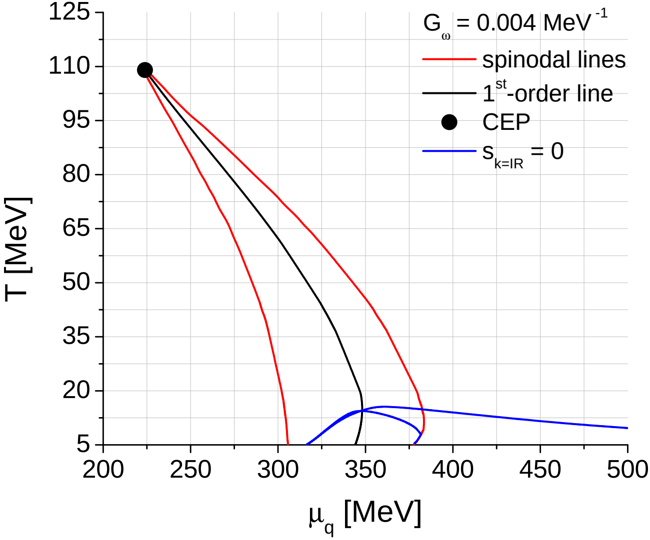

Phase Diagram: $k_{\rm IR} = 80$ MeV

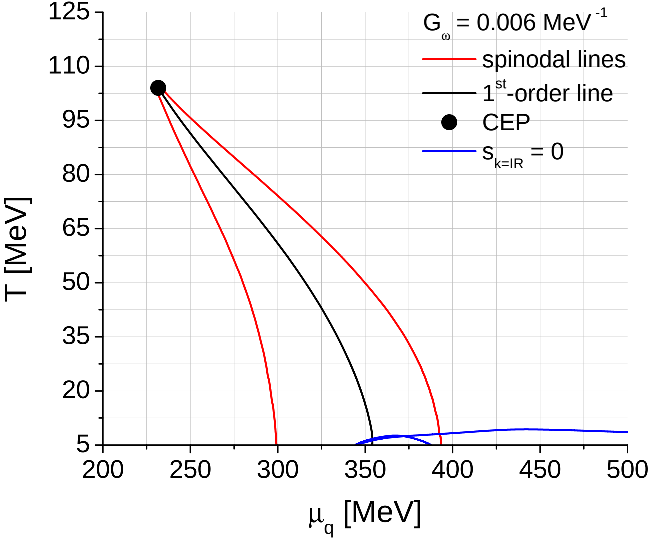

Phase Diagram: $k_{\text{IR}} = 80$ MeV

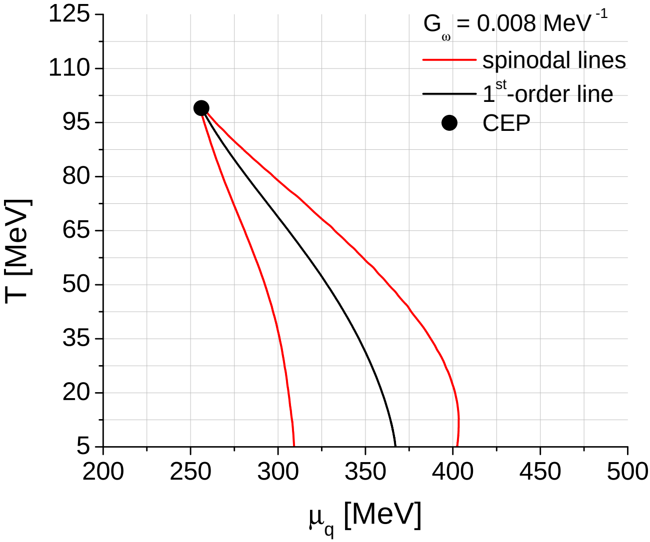

Phase Diagram: $k_{\rm IR} = 80$ MeV

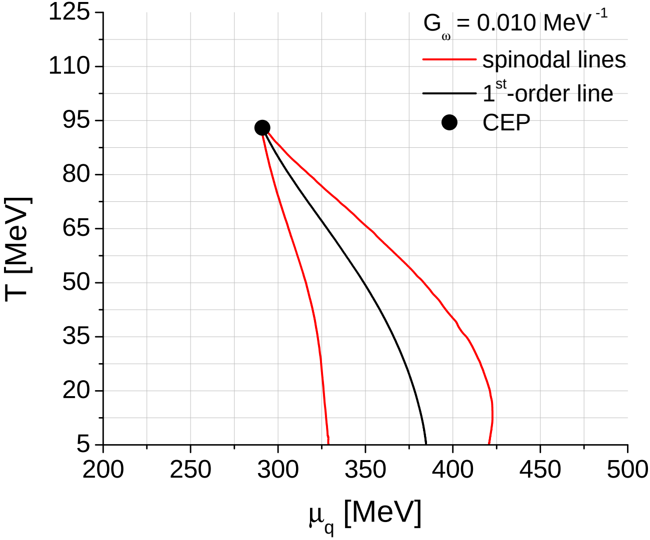

Phase Diagram: $k_{\text{IR}} = 80$ MeV

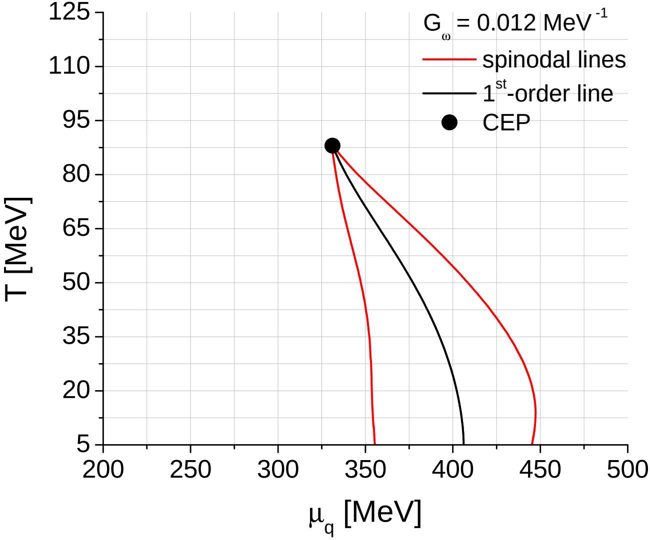

Phase Diagram: $k_{\mathrm{IR}} = 80$ MeV

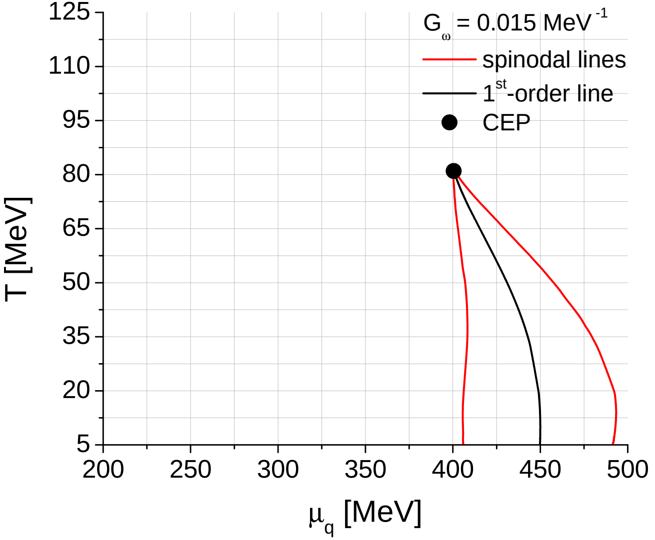

Conclusions

- The line $s_{k_{\rm IR}} = 0$ is an isentropic line;
- The behaviour of the critical region under finite vector interactions is very different from mean field calculations;
- The critical region is very narrow, but it gets larger for increasing G_ω;
- Increasing the coupling G_ω, drives the unphysical $s_{k_{\rm IR}} < 0$ region, towards smaller values of T and higher values of μ_q;

Further Work

- Study systems in $\beta-$equilibrium with zero eletric charge (neutron star matter);
- Explore the effect of different UV potentials as initial conditions for the flow;
- Explore the effect of different interactions (e.g. diquark-quark channels);
- Go beyond the LPA approximation and use different regulator functions;

Thank you for your attention!

This work is funded by National funds through FCT-IDPASC Portugal Ph.D. program under the grant PD/BD/128234/2016 and the project UID/FIS/-04564/2016.

This work was started during a STSM, in the scope of the COST Action CA16214, *"PHAROS: The multi-messenger physics and astrophysics of neutron stars"*, at the INFN - Sezione di Torino with Dr. Rainer Stiele.

References

Ralf-Arno Tripolt et al. "Low-temperature behavior of the quark-meson model." In: *Phys. Rev.* D97.3 (2018), p. 034022. DOI: 10.1103/PhysRevD.97.034022. arXiv: 1709.05991 [hep-ph].

G. G. Barnafoldi, A. Jakovac, and P. Posfay. "Harmonic expansion of the effective potential in a functional renormalization group at finite chemical potential." In: *Phys. Rev.* D95.2 (2017), p. 025004. DOI: 10.1103/PhysRevD.95.025004. arXiv: 1604.01717 [hep-th].

Thermodynamics

After calculating Γ, several thermodynamic quantities of interest, can be derived:

$$
\begin{aligned}
P(T,\mu) - P_0 &= -\Gamma(T,\mu),\\
\rho_i(T,\mu) &= -\left(\frac{\partial \Gamma(T,\mu)}{\partial \mu_i}\right)_T,\\
s(T,\mu) &= -\left(\frac{\partial \Gamma(T,\mu)}{\partial T}\right)_\mu,\\
\epsilon(T,\mu) &= -P(T,\mu) + Ts(T,\mu) + \sum_i \mu_i \rho_i(T,\mu).
\end{aligned}
$$

The constants P_0 and ϵ_0 are the pressure and energy density in the vacuum, respectively.

To derive the flow equation, some approximation scheme must be employed. We will consider the Local Potential Approximation (LPA): an operator expansion with increasing mass dimension.

In the lowest order of LPA, only the potential is scale dependent and the average effective action is:

$$\Gamma_k[T,\tilde{\mu}] = \int_0^{1/T} \mathrm{d}\tau \int \mathrm{d}^3 x \left\{ \overline{\psi}\left[\partial\!\!\!/ + g_S(\sigma + i\boldsymbol{\tau}\cdot\boldsymbol{\pi}\gamma_5) - \tilde{\mu}\gamma_0\right]\psi + \frac{1}{2}(\partial_\mu\sigma)^2 + \frac{1}{2}(\partial_\mu\boldsymbol{\pi})^2 + \tilde{U}_k(\sigma,\boldsymbol{\pi},\omega_0)\right\}.$$

Choosing a regulator function, R_k and plugging the above equation into the Wetterich equations, leads to the flow equation.

Flow Equations: Entropy

We are also interested in studying the entropy of the system including quantum fluctuations.

The following dimensionful flow equation for the average entropy $s_k(T, \tilde{\mu}; \sigma)$ can be derived:

$$\partial_t s_k^{\chi}(T,\mu;\sigma) = -\frac{k^5}{12\pi^2}\Bigg\{ 2n_{\mathrm{B}}(E_\sigma)[1+n_{\mathrm{B}}(E_\sigma)]\left[\frac{1}{T^2} + \frac{\partial_\sigma^2 s_k^{\chi}}{2TE_\sigma^2}\right] + \partial_\sigma^2 s_k^{\chi}\frac{[1+2n_{\mathrm{B}}(E_\sigma)]}{2E_\sigma^3}$$

$$+6n_{\mathrm{B}}(E_\pi)[1+n_{\mathrm{B}}(E_\pi)]\left[\frac{1}{T^2} + \frac{\partial_\sigma s_k^{\chi}}{2\sigma TE_\pi^2}\right] + 3\partial_\sigma s_k^{\chi}\frac{[1+2n_{\mathrm{B}}(E_\pi)]}{2\sigma E_\pi^3}$$

$$+\frac{4N_c}{E_\psi}\sum_{i=u,d}\sum_{\eta=\pm 1}\frac{n_{\mathrm{F}}(E_\psi-\eta\tilde{\mu}_{k,i})}{T^2}[1-n_{\mathrm{F}}(E_\psi-\eta\tilde{\mu}_{k,i})][E_\psi-\eta\tilde{\mu}_{k,i}-\eta T\partial_T g_\omega\tilde{\omega}_{0,k}]\Bigg\}.$$